Title: Electrochemical Phase Interconversion Enables Homogeneous-Heterogeneous Bifunctionality in Pd-Catalyzed Vinyl Acetate Synthesis

Authors: Deiaa M. Harraz[1†], Kunal Lodaya[1†], Bryan Y. Tang[2], and Yogesh Surendranath[1*]

[†]Denotes equal contribution
*Corresponding author. Email: yogi@mit.edu

Affiliations:
[1]Department of Chemistry, Massachusetts Institute of Technology, Cambridge, Massachusetts 02139, United States
[2]Department of Chemistry and Chemical Biology, Harvard University, Cambridge, Massachusetts 02138, United States

Abstract:
Current mechanistic paradigms in catalysis generally hold that a catalytic cycle is carried out by either a homogeneous or heterogeneous active species. Herein, we show that a prominent industrial process, palladium-catalyzed vinyl acetate synthesis, proceeds via interconversion of heterogeneous Pd(0) and homogeneous Pd(II) during catalysis, with each species playing a complementary role. Using electrochemical probes, we find that heterogeneous nanoparticulate Pd(0) serves as an active oxygen reduction electrocatalyst to furnish the high driving force required for corrosion to form homogeneous Pd(II), which then catalyzes selective ethylene acetoxylation with re-formation of heterogeneous Pd(0). Inhibiting the corrosion of Pd(0) to Pd(II) by galvanic protection results in reversible poisoning of catalysis, highlighting the essential role of phase conversion in this catalytic cycle. These results challenge the tacit assumption that catalysis proceeds via either homogeneous or heterogeneous modes, and instead highlights how dynamic phase interconversion can serve to harness and couple complementary reactivity across molecular and material active sites.

One-Sentence Summary:
Electrochemical analysis reveals that Pd catalyzed vinyl acetate synthesis proceeds via on-cycle interconversion of metallic Pd and homogeneous Pd(II), with each species playing a complementary role in the catalytic cycle.

Main text:

Electrochemical Phase Interconversion Enables Homogeneous-Heterogeneous Bifunctionality in Pd-Catalyzed Vinyl Acetate Synthesis

Mechanistic paradigms for catalysis have been broadly subdivided into two categories: heterogeneous catalysis and homogeneous catalysis. Heterogeneous catalytic mechanisms invoke chemical transformations at the interface between a solid catalyst and a liquid or gas phase that hosts the reactants. Homogeneous catalysis mechanisms instead invoke the action of soluble molecular species that bind and transform reactants. These distinct modes of catalysis engender distinct catalyst design principles. Ligand design is a cornerstone of homogeneous catalysis, while control of surface structure is central to heterogeneous catalysis.[1,2] Correspondingly, distinct research communities have gathered around designing and investigating catalysis with either a homogeneous or heterogeneous mode of action in mind.

It has long been appreciated that heterogeneous materials can serve as pre-catalysts for homogeneous active phases, and vice versa.[3] For example, in the discovery of olefin hydroformylation, catalysis was initially ascribed to heterogeneous cobalt metal before it was realized that homogeneous Co(I) species form in-situ and catalyze the reaction.[4] On the other hand, homogeneous Co(II) is a well-known precatalyst for heterogeneous cobalt oxide species that catalyze water oxidation.[5–7] This question is particularly poignant for Pd catalysis, for which there is ongoing debate on the active phases responsible for the wide array of transformations.[8–10] For example, in numerous Pd catalyzed cross couplings, heterogeneous metallic Pd catalysts have been employed, but growing evidence points to the metallic Pd serving as a pre-catalyst for homogeneous Pd(II) complexes that are responsible for catalytic turnover, as illustrated generically in **Figure 1A**.[11–13] Similarly, it has been recognized that homogeneous Pd(II) species can serve as pre-catalysts to metallic Pd active phases (**Figure 1B**).[14] Critically, in all of these examples, material-molecule or molecule-material interconversion is invoked to occur prior to steady-state turnover to generate the active phase. Consequently, catalysis is thought to proceed entirely via a homogeneous or heterogeneous mechanism, after the phase conversion, as illustrated in **Figure 1A and Figure 1B**. Thus, while molecule-material transformations may be required for entry into the catalytic cycle, to our knowledge, these transformations are not invoked to be part of the catalytic cycle itself.

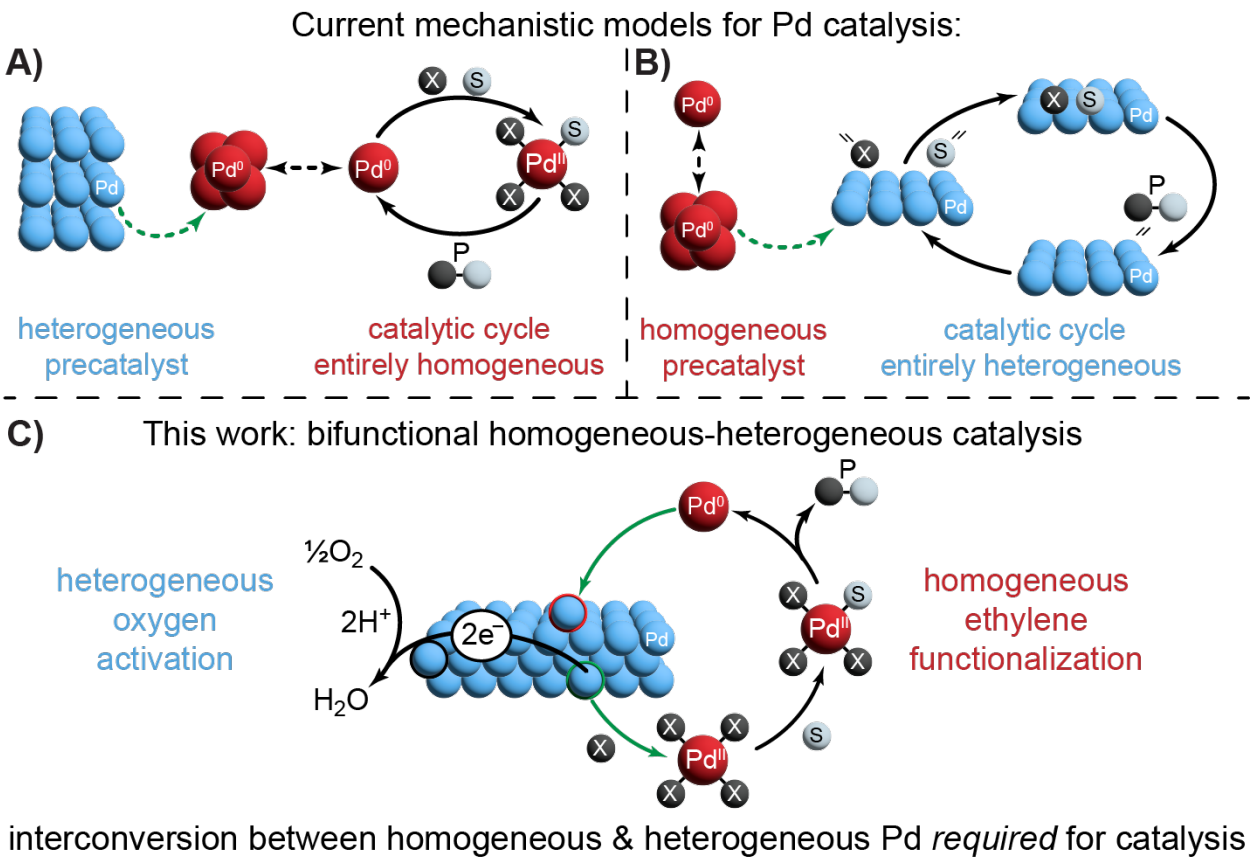

Fig. 1. **Schematic models for the role of phase conversion in Pd catalysis.** Top: phase conversion is external to the catalytic cycle and serves to form homogeneous (left) or heterogeneous (right) active catalytic species. Bottom: phase conversion is on-pathway in the catalytic cycle, and interconversion is required for catalysis, with each phase playing a complementary role. P and S represent generic product and reactant species, X represents a generic ligand species.

As an alternative to the above legacy paradigms, it is possible that a catalytic sequence could proceed through the dynamic interconversion of homogeneous and heterogeneous active phases as part of the catalytic cycle, as depicted in **Figure 1C**. In such a sequence, catalyst speciation is dynamic and may take advantage of complementary functions provided by heterogeneous and homogeneous species. Evidence in support of the dynamic interconversion of homogeneous and heterogeneous species during turnover could serve to bridge these traditionally disparate subdisciplines of catalysis and expose new opportunities for mechanistic understanding and catalyst design.

A prominent industrial catalytic process for which both homogeneous and heterogeneous mechanisms have been proposed is the aerobic oxidation of ethylene in the presence of acetic acid, to form vinyl acetate (VA).[15] This reaction is performed with a vapor phase reactant feed over supported Pd or Pd alloy catalysts with alkali acetate promoters. Despite decades of industrial implementation of Pd catalysts for VA synthesis, and decades of academic research, the mechanism for this reaction remains poorly understood. Many insights into VA synthesis have been accrued from studies of model single crystal surfaces.[16–19] Indeed, these spectroscopic and kinetic studies on model Pd surfaces have provided evidence for the formation of a surface acetoxyethyl intermediate which undergoes β-hydride elimination to form VA,[18] paralleling the mechanistic

steps invoked for molecular Pd complexes in homogeneous catalysis. Further studies on model single-crystal catalyst surfaces have suggested that a pair of palladium atoms are required to furnish the active site.[17] These findings have led to a heterogeneous mechanistic picture involving: surface adsorption, recombination of acetate and olefin adsorbates, β-hydride elimination, and scavenging of the generated surface hydrogen by O_2.[20,21] Importantly, this sequence invokes classical Langmuir–Hinshelwood, or Eley–Rideal mechanistic steps in an entirely heterogenous catalytic cycle.

The conditions of industrial VA synthesis differ dramatically from the foregoing model studies. In particular, industrial VA synthesis occurs at much higher pressures, utilizes alkali acetate promoters, and is conducted on Pd nanoparticles hosted on hydrophilic supports. While the conditions of model surface science studies may inhibit the formation of liquid phases, the reaction conditions typically employed for VA synthesis are known to foster the formation of thin liquid films on the catalyst surface that consist of acetic acid, water, and alkali salts.[22–25] Given the presence of a liquid phase during reaction conditions, and the well-established oxidative olefin functionalization chemistry of molecular Pd(II) complexes, some authors have proposed an entirely homogeneous mechanism for vinyl acetate synthesis.[22,26] In this mechanism, soluble Pd(II) in the liquid film is invoked to couple ethylene and acetic acid to produce molecular Pd(0) and vinyl acetate. This proposed mechanism parallels the Wacker process,[15,27,28] which is an industrial oxidation of ethylene to acetaldehyde by a homogeneous Pd(II) catalyst. For such homogeneous oxidative functionalization reactions involving Pd(II)/Pd(0) redox cycles, the molecular Pd(0) intermediate must be efficiently re-oxidized to minimize Pd(0) aggregation and subsequent deactivation.[9,29] Rapid reoxidation of molecular Pd(0) is furnished by a Cu co-catalyst in the Wacker process,[30] and benzoquinone has been employed as a oxidant in place of O_2 in examples of homogeneous liquid phase VA synthesis.[27,31] However, the conditions of industrial VA synthesis lack quinone or Cu-based oxidants that are effective for turnover of homogeneous Pd(II)/Pd(0) cycles. Thus, invoking a purely homogeneous cycle for aerobic VA synthesis requires that O_2 directly re-oxidize molecular Pd(0). However, re-oxidation of Pd(0) by O_2 is known to be challenging, particularly relative to aggregation of molecular Pd(0) species to form bulk Pd metal precipitates (also referred to as Pd black).[29,32,9] Consequently, the formation of metallic Pd is generally viewed as a catalytic dead end in aerobic oxidation reactions. Given the lack of classical co-oxidants critical for turnover of Wacker-type cycles, many mechanistic proposals have overlooked molecular Pd(II) species as relevant intermediates in VA synthesis. Rather, many other roles have been ascribed to Pd(II), ranging from Pd(II) being a spectator species correlated with catalyst deactivation, to Pd(II) causing nonselective ethylene oxidation to acetaldehyde, or Pd(II) serving to restructure the heterogeneous Pd surface to promote an entirely heterogeneous catalytic cycle.[15,25,33,34] As the foregoing discussion highlights, legacy thinking in the context of VA synthesis has considered entirely homogeneous and heterogeneous mechanisms but has largely ignored the possibility of dynamic interplay or bifunctional synergy between the two.

Herein, we employ electrochemical probes to analyze the role of homogeneous and heterogeneous catalysis in Pd catalyzed vinyl acetate synthesis. We find that thermochemical VA synthesis is driven by underlying spontaneous polarization of supported Pd nanoparticles by O_2 to form Pd(II) acetate, which mediates selective oxidation of ethylene to VA, with re-deposition of Pd(0). In a model liquid phase acetic acid/acetate system, we find that exposure of Pd/C to O_2 leads to corrosion to form Pd(II) acetate and subsequent exposure to C_2H_4 yields stoichiometric production of VA with precipitation of Pd black. We further find that electrochemical Pd corrosion, electrocatalytic VA synthesis in the absence of O_2, and thermocatalytic aerobic VA synthesis, all

proceed at comparable potentials and display a common rate-potential scaling. Furthermore, the same catalyst potential range and rate-potential scaling is also observed during more industrially relevant vapor phase VA synthesis conditions. Finally, inhibiting Pd corrosion via galvanic protection serves to reversibly inhibit VA synthesis in both the bulk liquid and vapor phase. These observations point to a common mechanistic sequence in both bulk liquid and in the vapor phase, in which heterogeneous Pd catalysis of electrochemical O_2 reduction provides the high driving force necessary to electrochemically oxidize Pd metal to form molecular Pd(II) acetate, which then carries out a homogeneous coupling of ethylene and acetic acid, with reformation of Pd metal. In this model, the net aerobic oxidation catalysis involves a bifunctional synergy between homogeneous and heterogenous components which are coupled electrochemically to each other to furnish the overall transformation. By highlighting the critical role of dynamic material-molecule interconversion in VA synthesis, these findings challenge the legacy paradigm that catalysis proceeds entirely through one modality or another, exposing the largely untapped opportunities for design that leverage synergies between homogeneous and heterogeneous catalysis.

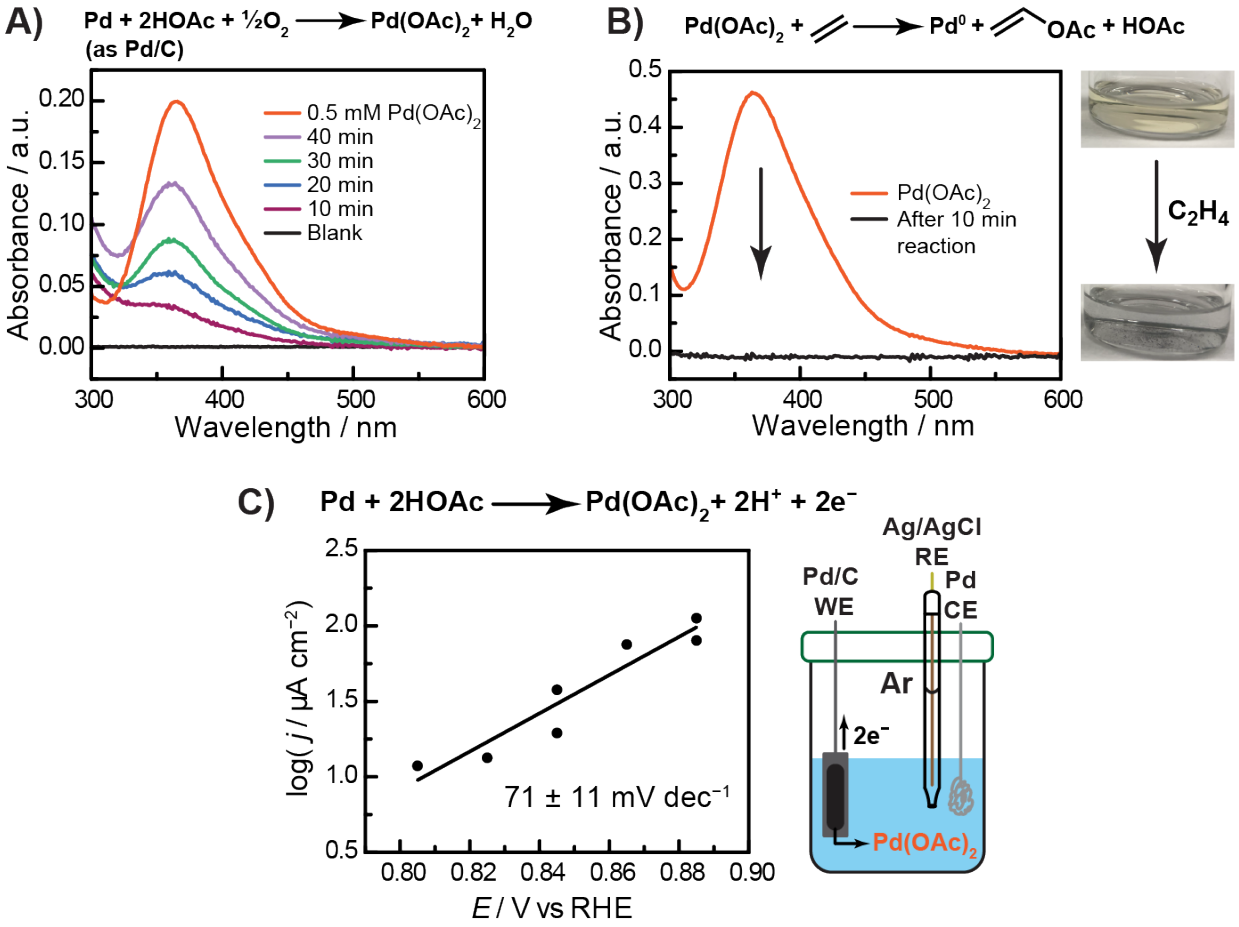

Figure 2. **Aerobic and electrochemical corrosion of Pd in acetic acid/acetate media. (A)** UV-Vis spectra over time of a glacial acetic acid with 0.5 M KOAc solution during aerobic corrosion of Pd/C in an atmosphere of 0.2 atm O_2 and 0.8 atm Ar **(B)** UV-Vis spectra (left) and photographs (right) of $Pd(OAc)_2$ in glacial acetic acid with 0.5 M KOAc prior to and following exposure to ethylene. **(C)** Cell schematic (right) and rate vs potential plot (left) for electrochemical corrosion of Pd/C to form Pd(II) in glacial acetic acid with 0.5 M KOAc. All data collected at 80 °C. Each data point in (C) represents a single measurement, and the line represents a linear fit of all data points. The rate-potential scaling is reported as the slope of this linear fit with standard error.

To study the chemistry of metallic palladium in an environment akin to the interfacial wetting layer formed during industrial catalysis, we employed a model bulk liquid phase medium consisting of glacial acetic acid with concentrated potassium acetate (0.5 M KOAc). We began our studies with Pd/C catalysts, to understand whether this carbon-supported nanoparticulate Pd metal phase could transform into solubilized Pd salts under these conditions. At 80 °C in the presence of 0.2 atm O_2 (balance Ar) we observe the gradual appearance of a yellow-orange colored species in solution over the course of 40 minutes with a UV-Vis peak absorbance at 365 nm (**Figure 2A**). The UV-Vis spectrum of the formed species matches that of authentic Pd(II) acetate solubilized in the same medium, and is diagnostic of Pd(II) bridging acetate dimers, the dominant speciation in acetic acid media with concentrated alkali acetates.[34] These findings are consistent with aerobic corrosion of Pd/C in the medium investigated. Exposure of these Pd(II) acetate solutions (formed from

corrosion, or prepared independently from commercial Pd(II) acetate) to ethylene results in a rapid loss of color within minutes, resulting in the precipitation of a metallic black solid (**Figure 2B**). ^{1}H NMR analysis of the resulting solution reveals the production of vinyl acetate from Pd(II) acetate with near quantitative yield (**Figure S1)**, consistent with prior observations.[27] Taken together, these two reactions represent – in net – the aerobic oxidation of ethylene to vinyl acetate. Moreover, this sequence demonstrates that it is possible to temporally separate VA synthesis into distinct components: a heterogeneous process for aerobic corrosion of Pd/C to form Pd(II) acetate, and the homogeneous reaction of Pd(II) acetate with ethylene to furnish vinyl acetate and metallic Pd^0 in the form of Pd black. Indeed, when Pd/C is exposed to both ethylene and O_2, catalytic VA synthesis is observed, producing 3.3 turnovers per Pd in 4 hours (**Figure S2**). In contrast, if we expose Pd black (obtained by exposing Pd(II) to ethylene in acetic acid/acetate medium) to the same conditions, only 0.6 turnovers per Pd are observed over the same time. (**Figure S2**). This observation suggests that Pd/C is subject to more efficient aerobic corrosion than the unsupported Pd black formed from reaction of Pd(II) with ethylene, leading us to further investigate aerobic corrosion of carbon-supported Pd in this medium.

Aerobic corrosion processes occur via coupling of an anodic metal corrosion electrochemical half-reaction, and a cathodic oxygen reduction electrochemical half-reaction (ORR).[35] This coupling of opposing half-reactions serves to establish an electrochemical mixed potential that characterizes the corrosion reaction. To measure the electrochemical potential of Pd/C during aerobic corrosion in acetic acid, we employed a two-electrode setup. Pd/C deposited onto carbon paper served as our working electrode, alongside an Ag/AgCl reference electrode positioned in the same reaction solution. Under the same aerobic corrosion conditions that produced Pd(II) acetate in the above experiments (20% O_2 in Ar, 80 °C) we observe the open circuit potential (OCP) of Pd/C equilibrates to ~0.90 V (**Figure S3**) (unless otherwise stated, all potentials are referenced to the reversible hydrogen electrode (RHE) potential under the conditions of the measurement). Upon varying the composition of O_2 in the headspace, from 5% to 20%, we observe the potential of Pd/C monotonically increases from approximately 0.84 to 0.90 V (**Figure S4**). This observation is in line with a classical corrosion mechanism, in which elevated O_2 pressure enhances the rate of oxygen reduction, resulting in a more oxidizing (higher potential) surface that drives more rapid conversion of Pd metal to Pd(II) acetate.

In order to individually investigate the constitutive ORR and Pd oxidation half-reactions of overall aerobic Pd corrosion, we constructed a three-electrode electrochemical cell, adding a Pd wire counter electrode to the existing two-electrode setup. Under a 20% O_2 in Ar headspace, we observe reductive current upon sweeping negatively from the OCP of 0.90 V diagnostic of oxygen reduction catalysis, and we observe anodic current above the OCP both in the presence and the absence of O_2 (**Figure S5)**. Constant potential electrolysis under Ar at 0.81 V leads to steady-state anodic current of 12 μA cm^{-2}, which rises to 96 μA cm^{-2} at an applied potential of 0.89 V (**Figure 2C**). Subsequent analysis of these solutions following electrolysis reveals near quantitative formation of Pd(II) acetate, equivalent to 2 electrons passed per Pd(II) ion formed (**Figure S6**). Importantly, the potential range over which we observe steady-state electrochemical corrosion of Pd(II) is in line with the potential range that the Pd/C electrode experiences over the span of O_2 partial pressures examined above (0.84–0.90 V). Notably, steady state corrosion currents (normalized by geometric electrode area) on a polycrystalline Pd foil are substantially lower by a factor of ~200 relative to a Pd/C electrode at the same potential (**Figure S7**). While much of this attenuation likely results from the lower Pd surface area on polycrystalline Pd relative to Pd/C, it is also possible that the specific rate of Pd nanoparticle/nanocluster corrosion for Pd/C is enhanced

relative to bulk Pd.[36] Irrespective of precise cause, the attenuated rate of Pd corrosion half-reaction on Pd foil relative to Pd/C would be expected to shift the OCP during net aerobic corrosion to more positive values (see SI Section 4.1 for further discussion). Yet, we observe the opposite; the OCP of a Pd foil under O_2 is ~100 mV negative of that for a Pd/C electrode (**Figure S3**). This observation implies that the attenuation in the rate of the Pd corrosion half-reaction for low surface area Pd foil is also accompanied by an even greater attenuation in the rate of O_2 reduction, relative to Pd/C. These findings, taken together, establish that the dominant oxidative process at a Pd surface under O_2 in this medium is Pd corrosion to Pd(II) acetate and suggest that more facile aerobic corrosion on Pd/C relative to bulk Pd accrues from a combination of enhanced O_2 reduction and Pd oxidation rates. Furthermore, these electrochemical measurements also return a quantitative relationship between the applied potential and the rate of Pd(II) acetate formation; this log-linear relationship has a slope of 71 ± 11 mV dec^{-1} (decade in rate) at 80 °C (**Figure 2C**), demonstrating a sensitive potential dependence for the Pd oxidation half-reaction.

The foregoing observations highlight several key attributes of Pd/C corrosion in acetic acid/acetate electrolytes: First, Pd/C is an active ORR catalyst under these conditions, providing a high driving force for Pd oxidation. Indeed, the observed potentials are ~200 mV positive of the estimated thermodynamic potential of the O_2/H_2O_2 couple of 0.70 V,[37] suggesting that the Pd/C is principally carrying out four-electron O_2 reduction, in stark contrast to the aerobic oxidation of molecular Pd(0), which typically couples to the two-electron reduction of O_2 to H_2O_2.[29] Second, the high dispersion of Pd on Pd/C serves to promote both ORR and Pd corrosion relative to bulk Pd foils, allowing for efficient aerobic corrosion for supported Pd/C. These findings rationalize why VA synthesis is sluggish on the unsupported Pd black formed from the reaction of Pd(II) with ethylene. Third, the Pd surface is immune to oxidative passivation in the acetic acid/acetate medium. Indeed, in aqueous media, Pd is not subject to substantial anodic corrosion to Pd(II) ions and instead self-passivates via the formation of insoluble oxide surface layers.[38] The foregoing data indicate that this passivation is inhibited in acetic acid/acetate, likely due to the lower water activity in the concentrated acetic acid electrolyte. The finding that Pd/C is subject to both aerobic and electrolytic corrosion at comparable potentials led us to consider the entire reaction sequence of vinyl acetate synthesis from an electrochemical perspective.

Electrolytic VA synthesis and thermochemical VA synthesis share a common corrosion-driven mechanism

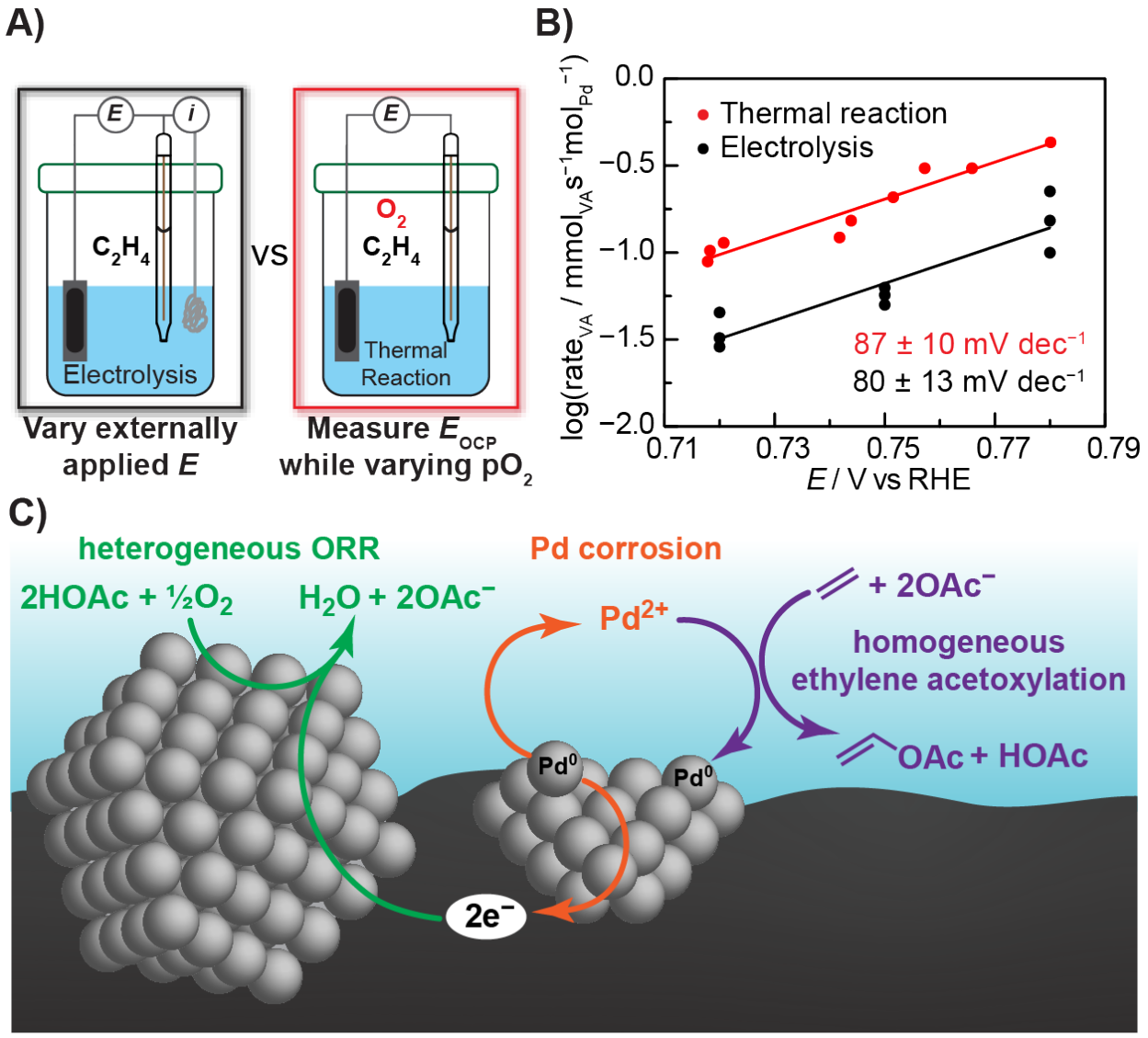

Figure 3. **Electrochemical and thermochemical vinyl acetate synthesis exhibit common rate-potential scaling. (A)** Comparison of experimental setup for electrolytic vinyl acetate synthesis (black box) and thermochemical vinyl acetate synthesis (red box) in glacial acetic acid with 0.5 M KOAc. **(B)** Rate vs potential plot and linear fit for electrolytic (red) and thermochemical (black) vinyl acetate synthesis in a common potential window, conducted at 80 °C. Each data point represents a single-point measurement of rate by measuring the amount of vinyl acetate formed following reaction via ^{1}H NMR. **(C)** Proposed mechanistic model for vinyl acetate synthesis, consisting of coupled oxygen reduction and Pd corrosion half-reactions at heterogeneous Pd sites followed by ethylene acetoxylation catalyzed by homogeneous Pd(II) species in solution.

Given that Pd(II) is a competent intermediate for VA synthesis and Pd/C is subject to electrolytic corrosion, we posited that VA could be produced electrocatalytically, in the absence of O_2. Indeed, a 1982 patent claimed electrochemical vinyl acetate synthesis at moderate FE, but with minimal experimental details and supporting data.[39] We set out to investigate the possibility of VA synthesis in the absence of O_2 by constructing an electrochemical cell and anodically polarizing a Pd/C

working electrode under a headspace of Ar and ethylene, and measuring VA formation rates by ^{1}H NMR (**Figure 3A**, left). Positive polarization of the Pd/C electrode in the presence of an C_2H_4/Ar atmosphere led to steady state production of VA. At an applied potential of 0.72 V, we observe a VA formation rate of 0.045 $mmol_{VA}/(s\ mol_{Pd})$ which rises to 0.22 $mmol_{VA}/(s\ mol_{Pd})$ at an applied potential of 0.78 V (**Figure 3B**, black). Across this range of applied potentials, we observe FE values >80% as quantified by ^{1}H NMR (**Figure S8)**, in line the high FEs observed for electrochemical corrosion and the quantitative selectivity of Pd(II) for ethylene acetoxylation. These findings establish that there is no *necessity* for O_2 in VA synthesis, and that externally-driven electrochemical polarization is sufficient for selective VA synthesis. Furthermore, we find that the logarithm of the rate of electrolytic VA synthesis is linearly correlated with applied potential, with a rate-potential scaling of 80 ± 13 mV dec^{-1}. Importantly, this scaling agrees with the rate-potential scaling of 71 ± 11 mV dec^{-1} observed for electrolytic Pd/C corrosion to Pd(II) acetate in the absence of both ethylene and O_2. This agreement suggests that during electrolytic VA synthesis, the active Pd(II) species is a homogeneous, solvated species, as observed during corrosion to form bulk Pd(II) in the liquid phase. This agreement also suggests that electrolytic VA synthesis proceeds through rate-controlling Pd corrosion followed by fast acetoxylation of ethylene by Pd(II) acetate.

To further probe this emerging mechanistic picture, we measured the open circuit potential of the Pd/C catalyst in the presence of both ethylene and O_2. We employed the same electrochemical cell and quantified VA production rates at 80 °C across a range of O_2 partial pressures while monitoring the OCP of the Pd/C catalyst (**Figure 3A**, right). We observed the OCP of the catalyst increase from 0.72 V to 0.78 V vs RHE, upon increasing the O_2 concentration in the headspace from 5% to 20%. As the measured potential of the catalyst rose with each increment in pO_2, we also observe a concomitant increase in the rate of VA production from 0.0080 mM min^{-1} at 0.72 V, to 0.039 mM min^{-1} at 0.78 V (**Figure 3B**, red). The data returns a rate-potential scaling of 87 ± 10 mV dec^{-1} at 80 °C, for *thermochemical O_2-driven* VA synthesis. Remarkably, this value agrees well with the rate-potential scaling of 80 ± 13 mV dec^{-1} for electrolytic VA synthesis, in which the oxidative driving force is provided by the external circuit rather than via the presence of O_2 (**Figure 3B**, red vs black). The absolute magnitudes of the rates are slightly higher during thermochemical VA synthesis, which we attribute to internal resistance within the thick Pd/C catalyst film on the electrode that serves to reduce the effective activity of VA electrocatalysis relative to thermochemical aerobic VA synthesis, since the latter requires no bulk current flow through the Pd/C film (see SI Section 4.2 and **Figure S14** for further discussion). Notwithstanding, the strong similarity in the polarization slopes implies that an electrochemical mechanism is operative in both cases and that the role of O_2 in thermochemical VA synthesis is to polarize the catalyst to a sufficiently high potential to elicit Pd corrosion.

Furthermore, this finding informs us that the kinetically relevant mode of Pd re-oxidation is a heterogeneous process, and not homogeneous re-oxidation of Pd(0) atoms or clusters in solution by O_2. Unlike for a heterogeneous corrosion, homogeneous re-oxidation of molecular Pd(0) by O_2 does not involve interfacial electron transfer, and thus should not give rise to an appreciable rate-potential scaling for the reaction. However, we observe the full rate-potential scaling for aerobic VA synthesis relative to electrolytic VA synthesis (**Figure 3B)**, informing us that the heterogeneous corrosion of Pd coupled to ORR is the kinetically relevant mode for Pd re-oxidation in VA synthesis. These data provide strong evidence against an entirely homogeneous, Wacker-type cycle for VA synthesis. Taken together, the foregoing studies point to the critical role of bifunctional

homogeneous-heterogeneous catalysis by Pd/C and Pd(II) acetate in the net thermochemical synthesis of VA, as illustrated in **Figure 3C**.

In such a sequence, heterogeneous Pd/C is positively polarized by O_2 via efficient electrocatalysis of the oxygen reduction reaction (**Figure 3C,** green**)**. This half-reaction is coupled to, and provides the driving force for, conversion of Pd nanoparticles on carbon to Pd(II) acetate via corrosion (**Figure 3C,** orange). Notably, there is no necessity for the same Pd sites to both activate O_2 and corrode to Pd(II); the presence of an ionically-conductive medium (acetic acid/acetate) and electronic conductivity (either through carbon, or through a single Pd nanoparticle) allows for these half-reactions to occur at disparate sites, akin to a local galvanic cell. In such a sequence, mixed-potential theory provides a framework to describe the rate of corrosion, and has been employed recently to describe a variety catalytic redox processes as well.[40–47] In such a local-cell mechanism, the heterogeneous Pd sites undergo spontaneous electrochemical polarization in the presence of O_2 to reach a steady-state potential (the "mixed potential"). At this potential, the rates of the coupled electrochemical half-reactions, oxygen reduction and Pd corrosion, are exactly balanced. The overall vinyl acetate synthesis involves additional steps after corrosion: the soluble Pd(II) produced via half-reaction coupling undergoes a homogeneous reaction with ethylene to form vinyl acetate and molecular Pd(0), which deposits on the surface to replenish the heterogeneous Pd (**Figure 3C,** violet). If the rate of the homogeneous reaction of Pd(II) was limiting in such a sequence, one would not observe a rate-potential scaling as the homogeneous reaction pathway does not involve interfacial charge transfer. The observation of a rate-potential scaling for thermochemical VA synthesis matching that of corrosion suggests that the overall rate of VA synthesis is controlled by the rate of corrosion.

Vapor phase vinyl acetate synthesis maintains the rate-potential scaling observed in the liquid phase

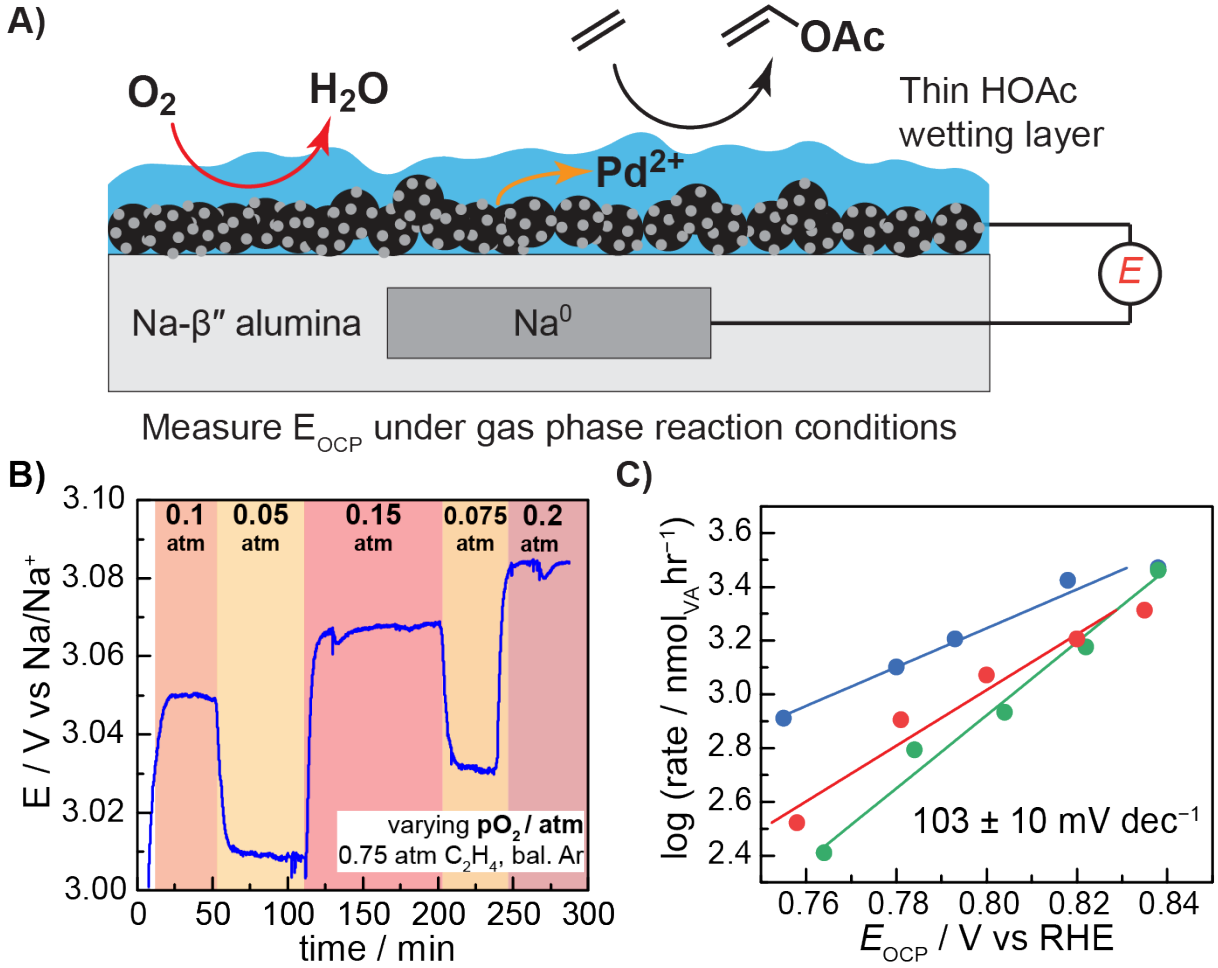

Figure 4. Potential and rate measurements in vapor phase synthesis conditions demonstrate comparable scaling to liquid phase measurements. (A) Scheme illustrating potential measurement of Pd/C during vapor phase vinyl acetate synthesis at 120 °C by solid electrolyte potentiometry. **(B)** Measurement of potentials of Pd/C as a function of gas composition; 75% ethylene, 5–20% O_2, balanced with Ar to 1 atm. Each condition was maintained for at least 45 minutes to ensure a stable potential was measured and to make at least three measurements of the vinyl acetate synthesis rate via online gas chromatography. **(C)**. Rate vs potential plot for vinyl acetate synthesis in vapor phase conditions on a solid-electrolyte reference probe. Measurements were conducted with a gas stream consisting of 75% ethylene, 5–20% O_2, balanced with Ar to 1 atm. Prior to being introduced to the reactor, the gas stream was bubbled through glacial acetic acid held at a constant temperature of 50 °C, introducing 0.076 atm acetic acid in the gas phase. The three colors (blue, red, and green) represent three replicate catalyst coated reference probes prepared with the same procedure, and each point represents a single-point measurement after reaching steady-state vinyl acetate synthesis rates. The reported rate-potential scaling is an average value of the rate-potential scaling values of the three replicate reference probes with one standard deviation.

The forgoing data implicate an electrochemical corrosion mechanism for VA synthesis in our model system employing a bulk acetic acid/acetate liquid phase. However, industrial Pd catalyzed VA synthesis does not occur in a bulk liquid phase, but instead employs a feed of acetic acid vapor that supports the formation of thin wetting layers on the catalyst surface.[22–25] Thus, the foregoing

findings raise the question of whether bifunctional homogeneous-heterogeneous catalysis and material-molecular interconversion are also operative under industrially relevant, higher temperature conditions. To probe this possibility, we sought to measure the potential of a Pd/C catalyst under the conditions of vapor phase catalysis. We employed a solid electrolyte potentiometry technique that allows us to measure the open circuit potential of a Pd/C catalyst film and relate this potential to bulk liquid phase potential measurements by referencing to RHE (See SI section 4.3 and **Figure S9** for further discussion). Briefly, we applied a coating of a NaOAc-promoted Pd/C catalyst onto the surface of a Na-β″ alumina solid electrolyte cylinder that houses an internal Na/Na^+ reference electrode (**Figure 4A**). This catalyst/solid electrolyte/reference electrode combination was enclosed in a reactor and exposed to a vapor input stream of the reactant gases. Under reaction conditions, we postulated that acetic acid could form a thin wetting layer akin to that which is formed on industrial catalysts, allowing us to measure the electrochemical potential of the Pd/C|HOAc/NaOAc interface. This HOAC/NaOAc wetting layer provides an electrolyte contact between the Pd/C catalyst and the solid electrolyte, providing a continuous pathway for ionic conduction between the catalyst and Na/Na^+ reference electrode. Upon introducing acetic acid vapor, ethylene and oxygen over a catalyst previously exposed to hydrogen (to measure the RHE potential) and argon, we observe a rapid polarization of the catalyst from 2.4 V to 3.05 V vs Na/Na^+, corresponding to a jump from 0.15 V to 0.8 V vs RHE under these conditions (**Figure S9**). Upon varying O_2 partial pressure at constant ethylene and acetic acid pressures (Ar balance), we observe rapid changes in the measured OCP of the catalyst. The OCP systematically increases with increasing pO_2, ranging from 0.76 to 0.84 V for a 0.05 atm to 0.2 atm pO_2 range (**Figure 4B**). Notably, this range of potentials is similar to the 0.84 to 0.90 V range observed in bulk liquid phase experiments over the similar pO_2 range, despite the higher temperature employed for vapor phase catalysis (120 °C vs 80 °C). This suggests that the Pd/C sites experience similar interfacial environments when exposed to either bulk liquid electrolyte or a vapor feed, due, presumably, to the spontaneous formation of a thin acetic acid film on the Pd/C film, as depicted in **Figure 4A**. These data evince that under the conditions of vapor phase vinyl acetate synthesis, the Pd catalyst experiences *spontaneous* polarization with respect to oxygen partial pressure with remarkable similarity to that observed in the presence of a bulk liquid phase.

The foregoing findings led us to further examine the possibility of a similar electrochemical mechanism for VA synthesis under vapor phase conditions. We measured the rate-potential scaling for vapor phase VA synthesis by varying the O_2 partial pressure, as we did when measuring the rate-potential scaling for thermal VA synthesis in the liquid phase (**Figure 3B**). Using the same Pd/C on Na-β″ alumina probes that were used to previously measure polarization of the catalyst film, we quantified the rate of VA synthesis. As the catalyst potential (due to increases in pO_2) increases from 0.76 to 0.84 V, we observed a concomitant increase in the average rate of VA synthesis increases from 470 nmol hr^{-1} to 2640 nmol hr^{-1} (**Figure 4C).** This corresponds to an average rate-potential scaling of 103 ± 10 mV dec^{-1} at 120 °C which when scaled to a reaction temperature of 80 °C by the Nernst equation, corresponds to a scaling of 93 ± 9 mV dec^{-1}, within error of the corresponding scale factors observed in the liquid phase for aerobic VA synthesis (**Figure 3B**, red), electrolytic VA synthesis (**Figure 3B**, black), and near the scale factor for electrolytic Pd corrosion (**Figure 2C**). Additionally, when the carbon film is removed from the β″ alumina probe, a grey metallic color remains on the surface of the β″ alumina which we attribute to Pd corrosion and redeposition under reaction conditions (**Figure S10**). Taken together, these data suggest a similar corrosion-mediated bifunctional mechanism is operative under both vapor phase and bulk liquid phase conditions.

Galvanic poisoning of palladium with aluminum inhibits catalysis

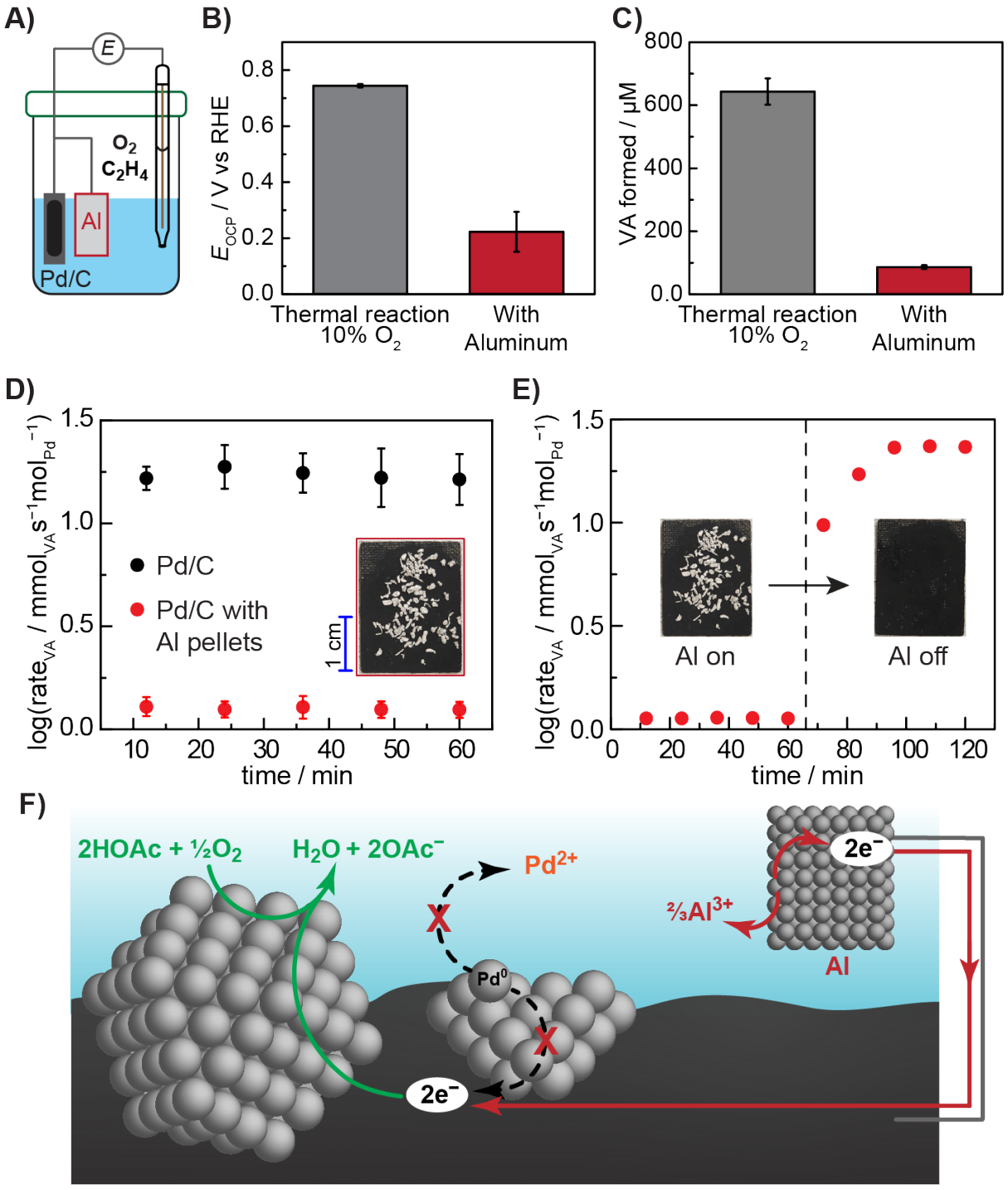

Figure 5. **Galvanic protection of palladium by aluminum during vinyl acetate synthesis. (A)** Experimental setup schematic for liquid phase galvanic protection in 0.5 M KOAc in glacial acetic acid at 80 °C. **(B)** Comparison of the open-circuit potential for Pd/C exposed to thermochemical vinyl acetate synthesis conditions of 75% ethylene, 10% O_2 and balance Ar (grey) and the same catalyst contacted to a strip of Al foil (red). **(C)** Comparison of the amount of vinyl acetate formed by Pd/C with and without contact to Al foil over the course of 1 hour, as determined by post-reaction analysis of the solution via ^{1}H

NMR. **(D)** Rate measurements at five time points for a Pd/C catalyst exposed to vapor phase vinyl acetate synthesis conditions (black) and under the same conditions following the addition of Al pellets (red). **(E)** Rate measurements before (left) and after (right) removing Al pellets from Pd/C catalyst under vapor phase vinyl acetate synthesis conditions. **(F)** Proposed mechanistic model for poisoning of vinyl acetate synthesis by galvanic protection with Al, with current flowing from Al to reduce O_2 at the Pd surface without concomitant oxidation of Pd to Pd(II). Vapor phase VA synthesis rates were measured at 120 °C with a gas stream consisting of 0.75 atm C_2H_4, 0.1 atm O_2, and balanced with Ar to 1 atm. This gas stream was bubbled through glacial acetic acid held at constant temperature of 50 °C, introducing 0.076 atm acetic acid in the gas phase. All data points and bars shown are the average of three measurements, with error bars representing one standard deviation.

While the results presented thus far have ruled out an entirely homogeneous pathway for Pd catalyzed aerobic VA synthesis, they cannot rule out the involvement of a purely heterogeneous pathway concurrent with the electrochemical mechanism proposed above. So-called "heterogeneity" tests have been widely employed to examine whether a particular Pd-catalyzed reaction is catalyzed by a heterogeneous Pd surface or a homogeneous molecular Pd catalyst.[8] These tests, which poison one catalytic phase or the other as part of a mechanistic analysis, have proven critical for assessing the active species in both Pd catalysis and other examples of catalysis.[48,49] However, in the electrochemical corrosion-based mechanism proposed here, both heterogeneous Pd and homogeneous Pd are explicitly required for catalysis, necessitating a different type of test than those previously employed that inhibit either heterogeneous or homogeneous Pd catalysis. We sought an experimental test that would not inhibit the catalytic activity of heterogeneous Pd, nor that of homogeneous Pd(II), but instead inhibit the interconversion of heterogeneous Pd to homogeneous Pd(II). Such a test, if successful at "poisoning" the catalyst, would serve to rule out a purely heterogeneous mechanism, taken together with our prior observations.

To establish such a test we employed galvanic protection, a classic strategy for corrosion inhibition, to selectively poison VA synthesis proceeding via heterogeneous Pd corrosion and subsequent homogeneous olefin acetoxylation. During galvanic protection, a thermodynamically (and kinetically) more corrodible metal is contacted with a more noble metal, and the more corrodible metal is oxidized in place of the noble metal during oxidative processes. This results in a cathodic shift of the mixed potential, and an attenuation in the oxidation rate of the more noble metal. We chose aluminum as the galvanic protectant, as it corrodes but not too rapidly in this medium, over the timescale of our experiments. We carried out thermochemical VA synthesis and measured catalyst potential while contacting the Pd/C catalyst electrode to a strip of high purity aluminum foil (**Figure 5A**). The Al foil was connected electrically to the Pd with minimal direct contact, so as to minimize physical blocking of Pd sites by the foil. The electrical contact to the Al foil manifests in an average decrease in catalyst potential from 0.74 V to 0.22 V, and a simultaneous depression in VA production by ~7-fold, as shown in **Figure 5B** and **Figure 5C** respectively. Further analysis reveals that the small amount of VA produced during the galvanic protection experiment is formed in the initial 15 minutes of the experiment, as the potential of the working electrode is still decreasing; afterwards, the steady state rate of VA production falls below the ^{1}H NMR detection limit (**Figure S11**). These observations are best explained by a galvanic poisoning of Pd/C by aluminum, illustrated in **Figure 5F**. The Pd/C in electronic contact with Al can still catalyze ORR, but the generated holes now go towards oxidizing the Al instead of the Pd, leading to lower mixed potential and complete attenuation of steady state VA synthesis rates. The lack of observable steady state VA production upon galvanic protection of Pd/C suggests that not only is

an electrochemical mechanism operative, but that it is indeed the dominant mechanism of VA synthesis. These data provide strong evidence against non-electrochemical mechanisms and indicate that entirely heterogeneous pathways are not significant contributors to VA production in the liquid phase under these conditions.

Aluminum is an effective galvanic poison for Pd catalyzed vinyl acetate synthesis not only in our bulk liquid phase model system, but also in the vapor phase reaction as well. In the liquid phase, the negative polarization provided by aluminum is achieved in a straightforward fashion by electrically connecting aluminum foil and a Pd/C electrode, both in contact with a common acetic acid electrolyte to furnish ionic conductivity. We envisioned that the spontaneously formed acetic acid/acetate wetting layer would also furnish conductivity between Al pellets and the Pd/C under vapor phase conditions. For vapor phase catalysis galvanic poisoning studies, we employed a carbon paper electrode impregnated with Pd/C, as this provided a conductive medium on which to also disperse aluminum pellets. With Pd/C on carbon paper alone, we observe stable VA synthesis over the course of 1 hour, with an average rate of 1.2 $mmol_{VA}/(s\ mol_{Pd})$ (**Figure 5D**, black). Next, we removed the carbon paper from the reactor and added aluminum to the catalyst in the form of macroscopic pellets (~1 mm diameter) sprinkled on top of the Pd/C film, and placed the carbon paper back into the reactor. Immediately, we observe the steady state rate of vapor phase VA synthesis decrease by an order of magnitude to 0.1 $mmol_{VA}/(s\ mol_{Pd})$ for Pd/C with aluminum pellets (**Figure 5D**, red). Remarkably, this rate reduction is reversible; upon scraping off the macroscopic Al particles, we observe the VA synthesis rate recover to the original value (**Figure 5E**). This demonstrates that under the conditions of vapor phase vinyl acetate synthesis, aluminum is a potent and reversible galvanic poison. These observations are most readily explained by invoking that the corrosion of Pd is required in the catalytic cycle.

Taken together, our observations are inconsistent with mechanisms for Pd catalyzed VA synthesis that invoke entirely homogeneous or heterogenous catalytic cycles. Rather, these results point to a mechanism in which catalyst phase conversion is an on-pathway process, required to furnish a bifunctional catalyst system in which heterogeneous Pd and homogeneous Pd(II) carry out complementary roles of oxygen reduction and olefin functionalization, respectively. These findings suggest a rich untapped opportunity to distribute the disparate burdens of a catalytic sequence across homogeneous and heterogeneous catalysts that act in concert to carry out efficient and selective catalysis.

References and Notes

(1) Herrmann, W. A.; Cornils, B. Organometallic Homogeneous Catalysis—Quo Vadis? *Angew. Chem. Int. Ed. Engl.* **1997**, *36* (10), 1048–1067. https://doi.org/10.1002/anie.199710481.

(2) Zaera, F. Designing Sites in Heterogeneous Catalysis: Are We Reaching Selectivities Competitive With Those of Homogeneous Catalysts? *Chem. Rev.* **2022**, *122* (9), 8594–8757. https://doi.org/10.1021/acs.chemrev.1c00905.

(3) Widegren, J. A.; Finke, R. G. A Review of the Problem of Distinguishing True Homogeneous Catalysis from Soluble or Other Metal-Particle Heterogeneous Catalysis under Reducing Conditions. *Journal of Molecular Catalysis A: Chemical* **2003**, *198* (1–2), 317–341. https://doi.org/10.1016/S1381-1169(02)00728-8.

(4) Cornils, B.; Herrmann, W. A.; Rasch, M. Otto Roelen, Pioneer in Industrial Homogeneous Catalysis. *Angew. Chem. Int. Ed. Engl.* **1994**, *33* (21), 2144–2163. https://doi.org/10.1002/anie.199421441.

(5) Kanan, M. W.; Nocera, D. G. In Situ Formation of an Oxygen-Evolving Catalyst in Neutral Water Containing Phosphate and Co^{2+}. *Science* **2008**, *321* (5892), 1072–1075. https://doi.org/10.1126/science.1162018.

(6) Brunschwig, B. S.; Chou, M. H.; Creutz, C.; Ghosh, P.; Sutin, N. Mechanisms of Water Oxidation to Oxygen: Cobalt(IV) as an Intermediate in the Aquocobalt(II)-Catalyzed Reaction. *J. Am. Chem. Soc.* **1983**, *105* (14), 4832–4833. https://doi.org/10.1021/ja00352a050.
(7) Folkman, S. J.; Soriano-Lopez, J.; Galán-Mascarós, J. R.; Finke, R. G. Electrochemically Driven Water-Oxidation Catalysis Beginning with Six Exemplary Cobalt Polyoxometalates: Is It Molecular, Homogeneous Catalysis or Electrode-Bound, Heterogeneous CoO_x Catalysis? *J. Am. Chem. Soc.* **2018**, *140* (38), 12040–12055. https://doi.org/10.1021/jacs.8b06303.
(8) Phan, N. T. S.; Van Der Sluys, M.; Jones, C. W. On the Nature of the Active Species in Palladium Catalyzed Mizoroki–Heck and Suzuki–Miyaura Couplings – Homogeneous or Heterogeneous Catalysis, A Critical Review. *Adv. Synth. Catal.* **2006**, *348* (6), 609–679. https://doi.org/10.1002/adsc.200505473.
(9) Li, M.-B.; Bäckvall, J.-E. Efficient Heterogeneous Palladium Catalysts in Oxidative Cascade Reactions. *Acc. Chem. Res.* **2021**, *54* (9), 2275–2286. https://doi.org/10.1021/acs.accounts.1c00122.
(10) Ernst, J. B.; Schwermann, C.; Yokota, G.; Tada, M.; Muratsugu, S.; Doltsinis, N. L.; Glorius, F. Molecular Adsorbates Switch on Heterogeneous Catalysis: Induction of Reactivity by N-Heterocyclic Carbenes. *J. Am. Chem. Soc.* **2017**, *139* (27), 9144–9147. https://doi.org/10.1021/jacs.7b05112.
(11) Cassol, C. C.; Umpierre, A. P.; Machado, G.; Wolke, S. I.; Dupont, J. The Role of Pd Nanoparticles in Ionic Liquid in the Heck Reaction. *J. Am. Chem. Soc.* **2005**, *127* (10), 3298–3299. https://doi.org/10.1021/ja0430043.
(12) Astruc, D. Palladium Nanoparticles as Efficient Green Homogeneous and Heterogeneous Carbon−Carbon Coupling Precatalysts: A Unifying View. *Inorg. Chem.* **2007**, *46* (6), 1884–1894. https://doi.org/10.1021/ic062183h.
(13) Sun, B.; Ning, L.; Zeng, H. C. Confirmation of Suzuki–Miyaura Cross-Coupling Reaction Mechanism through Synthetic Architecture of Nanocatalysts. *J. Am. Chem. Soc.* **2020**, *142* (32), 13823–13832. https://doi.org/10.1021/jacs.0c04804.
(14) Pun, D.; Diao, T.; Stahl, S. S. Aerobic Dehydrogenation of Cyclohexanone to Phenol Catalyzed by $Pd(TFA)_2$ /2-Dimethylaminopyridine: Evidence for the Role of Pd Nanoparticles. *J. Am. Chem. Soc.* **2013**, *135* (22), 8213–8221. https://doi.org/10.1021/ja403165u.
(15) Zha, Z.; Giannakakis, G.; Deshlahra, P. Catalytic Routes and Mechanisms for Vinyl Acetate Synthesis. In *Catalysis*; Spivey, J., Han, Y.-F., Shekhawat, D., Eds.; Royal Society of Chemistry: Cambridge, 2021; Vol. 33, pp 87–113. https://doi.org/10.1039/9781839163128-00087.
(16) Kumar, D.; Chen, M. S.; Goodman, D. W. Synthesis of Vinyl Acetate on Pd-Based Catalysts. *Catalysis Today* **2007**, *123* (1–4), 77–85. https://doi.org/10.1016/j.cattod.2007.01.050.
(17) Chen, M.; Kumar, D.; Yi, C.-W.; Goodman, D. W. The Promotional Effect of Gold in Catalysis by Palladium-Gold. *Science* **2005**, *310* (5746), 291–293. https://doi.org/10.1126/science.1115800.
(18) Stacchiola, D.; Calaza, F.; Burkholder, L.; Schwabacher, A. W.; Neurock, M.; Tysoe, W. T. Elucidation of the Reaction Mechanism for the Palladium-Catalyzed Synthesis of Vinyl Acetate. *Angew. Chem. Int. Ed.* **2005**, *44* (29), 4572–4574. https://doi.org/10.1002/anie.200500782.
(19) Stacchiola, D.; Calaza, F.; Burkholder, L.; Tysoe, W. T. Vinyl Acetate Formation by the Reaction of Ethylene with Acetate Species on Oxygen-Covered Pd(111). *J. Am. Chem. Soc.* **2004**, *126* (47), 15384–15385. https://doi.org/10.1021/ja044641w.
(20) Zha, Z.; Deshlahra, P. Mechanistic Framework and Effects of High Coverage in Vinyl Acetate Synthesis. *ACS Catal.* **2021**, *11* (3), 1841–1857. https://doi.org/10.1021/acscatal.0c03673.
(21) Calaza, F.; Stacchiola, D.; Neurock, M.; Tysoe, W. T. Kinetic Parameters for the Elementary Steps in the Palladium-Catalyzed Synthesis of Vinyl Acetate. *Catal Lett* **2010**, *138* (3–4), 135–142. https://doi.org/10.1007/s10562-010-0386-0.
(22) Samanos, B.; Boutry, P.; Montarnal, R. The Mechanism of Vinyl Acetate Formation by Gas-Phase Catalytic Ethylene Acetoxidation. *Journal of Catalysis* **1971**, *23* (1), 19–30. https://doi.org/10.1016/0021-9517(71)90019-4.
(23) Crathorne, E. A.; Macgowan, D.; Morris, S. R.; Rawlinson, A. P. Application of Isotopic Transient Kinetics to Vinyl Acetate Catalysis. *Journal of Catalysis* **1994**, *149* (2), 254–267. https://doi.org/10.1006/jcat.1994.1294.
(24) Provine, W. D.; Mills, P. L.; Lerou, J. J. Discovering the Role of Au and KOAc in the Catalysis of Vinyl Acetate Synthesis. In *Studies in Surface Science and Catalysis*; Elsevier, 1996; Vol. 101, pp 191–200. https://doi.org/10.1016/S0167-2991(96)80229-1.
(25) Jacobs, H. P.; Elias, W. C.; Heck, K. N.; Dean, D. P.; Dodson, J. J.; Zhang, W.; Arredondo, J. H.; Breckner, C. J.; Hong, K.; Botello, C. R.; Chen, L.; Mueller, S. G.; Alexander, S. R.; Miller, J. T.; Wong, M. S. Impregnation of KOAc on $PdAu/SiO_2$ Causes Pd-Acetate Formation and Metal Restructuring. *J. Mater. Chem. A* **2023**, *11* (13), 6918–6933. https://doi.org/10.1039/D3TA00820G.

(26) Augustine, S. M.; Blitz, J. P. The Use of DRIFTS-MS and Kinetic Studies to Determine the Role of Acetic Acid in the Palladium-Catalyzed Vapor-Phase Synthesis of Vinyl Acetate. *Journal of Catalysis* **1993**, *142* (1), 312–324. https://doi.org/10.1006/jcat.1993.1210.
(27) Moiseev, I. I.; Vargaftik, M. N.; Syrkin, Y. K. On the Mechanism of the Reaction of Palladium Salts with Olefins in Hydroxyl-Containing Solutions. *Doklady Akademii Nauk* **1960**, *133*, 377–380.
(28) Kragten, D. D.; Van Santen, R. A.; Neurock, M.; Lerou, J. J. A Density Functional Study of the Acetoxylation of Ethylene to Vinyl Acetate Catalyzed by Palladium Acetate. *J. Phys. Chem. A* **1999**, *103* (15), 2756–2765. https://doi.org/10.1021/jp982956q.
(29) Wang, D.; Weinstein, A. B.; White, P. B.; Stahl, S. S. Ligand-Promoted Palladium-Catalyzed Aerobic Oxidation Reactions. *Chem. Rev.* **2018**, *118* (5), 2636–2679. https://doi.org/10.1021/acs.chemrev.7b00334.
(30) Teles, J. H.; Partenheimer, W.; Jira, R.; Cavani, F.; Strukul, G.; Hage, R.; De Boer, J. W.; Gooßen, L.; Mamone, P.; Kholdeeva, O. A. Oxidation. In *Applied Homogeneous Catalysis with Organometallic Compounds*; Cornils, B., Herrmann, W. A., Beller, M., Paciello, R., Eds.; Wiley, 2017; pp 465–568. https://doi.org/10.1002/9783527651733.ch7.
(31) Grover, G. S.; Chaudhari, R. V. Kinetics of Oxidation of Ethylene to Vinyl Acetate Using a Homogeneous Palladium Complex Catalyst. *The Chemical Engineering Journal* **1986**, *32* (2), 93–99. https://doi.org/10.1016/0300-9467(86)80056-9.
(32) Salazar, C. A.; Flesch, K. N.; Haines, B. E.; Zhou, P. S.; Musaev, D. G.; Stahl, S. S. Tailored Quinones Support High-Turnover Pd Catalysts for Oxidative C–H Arylation with O_2. *Science* **2020**, *370* (6523), 1454–1460. https://doi.org/10.1126/science.abd1085.
(33) Hanrieder, E. K.; Jentys, A.; Lercher, J. A. Atomistic Engineering of Catalyst Precursors: Dynamic Reordering of PdAu Nanoparticles during Vinyl Acetate Synthesis Enhanced by Potassium Acetate. *ACS Catal.* **2015**, *5* (10), 5776–5786. https://doi.org/10.1021/acscatal.5b01140.
(34) Kragten, D. D.; Van Santen, R. A.; Crawford, M. K.; Provine, W. D.; Lerou, J. J. A Spectroscopic Study of the Homogeneous Catalytic Conversion of Ethylene to Vinyl Acetate by Palladium Acetate. *Inorg. Chem.* **1999**, *38* (2), 331–339. https://doi.org/10.1021/ic980399g.
(35) Mixed Potential Theory. In *Electrochemistry and Corrosion Science*; Perez, N., Ed.; Springer US: Boston, MA, 2004; pp 155–166. https://doi.org/10.1007/1-4020-7860-9_5.
(36) Shan, H.; Gao, W.; Xiong, Y.; Shi, F.; Yan, Y.; Ma, Y.; Shang, W.; Tao, P.; Song, C.; Deng, T.; Zhang, H.; Yang, D.; Pan, X.; Wu, J. Nanoscale Kinetics of Asymmetrical Corrosion in Core-Shell Nanoparticles. *Nat Commun* **2018**, *9* (1), 1011. https://doi.org/10.1038/s41467-018-03372-z.
(37) Bratsch, S. G. Standard Electrode Potentials and Temperature Coefficients in Water at 298.15 K. *Journal of Physical and Chemical Reference Data* **1989**, *18* (1), 1–21. https://doi.org/10.1063/1.555839.
(38) Tang, J.; Petri, M.; Kibler, L. A.; Kolb, D. M. Pd Deposition onto Au(111) Electrodes from Sulphuric Acid Solution. *Electrochimica Acta* **2005**, *51* (1), 125–132. https://doi.org/10.1016/j.electacta.2005.04.009.
(39) James E. Kuder. Electrochemical Production of Vinyl Acetate. 4383899.
(40) Daniel, I. T.; Kim, B.; Douthwaite, M.; Pattisson, S.; Lewis, R. J.; Cline, J.; Morgan, D. J.; Bethell, D.; Kiely, C. J.; McIntosh, S.; Hutchings, G. J. Electrochemical Polarization of Disparate Catalytic Sites Drives Thermochemical Rate Enhancement. *ACS Catal.* **2023**, *13* (21), 14189–14198. https://doi.org/10.1021/acscatal.3c03364.
(41) Fortunato, G. V.; Pizzutilo, E.; Katsounaros, I.; Göhl, D.; Lewis, R. J.; Mayrhofer, K. J. J.; Hutchings, G. J.; Freakley, S. J.; Ledendecker, M. Analysing the Relationship between the Fields of Thermo- and Electrocatalysis Taking Hydrogen Peroxide as a Case Study. *Nat Commun* **2022**, *13* (1), 1973. https://doi.org/10.1038/s41467-022-29536-6.
(42) Huang, X.; Akdim, O.; Douthwaite, M.; Wang, K.; Zhao, L.; Lewis, R. J.; Pattisson, S.; Daniel, I. T.; Miedziak, P. J.; Shaw, G.; Morgan, D. J.; Althahban, S. M.; Davies, T. E.; He, Q.; Wang, F.; Fu, J.; Bethell, D.; McIntosh, S.; Kiely, C. J.; Hutchings, G. J. Au–Pd Separation Enhances Bimetallic Catalysis of Alcohol Oxidation. *Nature* **2022**, *603* (7900), 271–275. https://doi.org/10.1038/s41586-022-04397-7.
(43) Adams, J. S.; Kromer, M. L.; Rodríguez-López, J.; Flaherty, D. W. Unifying Concepts in Electro- and Thermocatalysis toward Hydrogen Peroxide Production. *J. Am. Chem. Soc.* **2021**, *143* (21), 7940–7957. https://doi.org/10.1021/jacs.0c13399.
(44) Zhao, Y.; Adams, J. S.; Baby, A.; Kromer, M. L.; Flaherty, D. W.; Rodríguez-López, J. Electrochemical Screening of Au/Pt Catalysts for the Thermocatalytic Synthesis of Hydrogen Peroxide Based on Their Oxygen Reduction and Hydrogen Oxidation Activities Probed via Voltammetric Scanning Electrochemical Microscopy. *ACS Sustainable Chem. Eng.* **2022**, *10* (51), 17207–17220. https://doi.org/10.1021/acssuschemeng.2c05120.

(45) Howland, W. C.; Gerken, J. B.; Stahl, S. S.; Surendranath, Y. Thermal Hydroquinone Oxidation on Co/N-Doped Carbon Proceeds by a Band-Mediated Electrochemical Mechanism. *J. Am. Chem. Soc.* **2022**, *144* (25), 11253–11262. https://doi.org/10.1021/jacs.2c02746.
(46) Lodaya, K. M.; Tang, B. Y.; Bisbey, R. P.; Weng, S.; Westendorff, K. S.; Toh, W. L.; Ryu, J.; Román-Leshkov, Y.; Surendranath, Y. An Electrochemical Approach for Designing Thermochemical Bimetallic Nitrate Hydrogenation Catalysts. *Nat Catal* **2024**, *7* (3), 262–272. https://doi.org/10.1038/s41929-023-01094-0.
(47) Ryu, J.; Bregante, D. T.; Howland, W. C.; Bisbey, R. P.; Kaminsky, C. J.; Surendranath, Y. Thermochemical Aerobic Oxidation Catalysis in Water Can Be Analysed as Two Coupled Electrochemical Half-Reactions. *Nat Catal* **2021**, *4* (9), 742–752. https://doi.org/10.1038/s41929-021-00666-2.
(48) Bayram, E.; Finke, R. G. Quantitative 1,10-Phenanthroline Catalyst-Poisoning Kinetic Studies of Rh(0) Nanoparticle and Rh_4 Cluster Benzene Hydrogenation Catalysts: Estimates of the Poison $K_{association}$ Binding Constants, of the Equivalents of Poison Bound and of the Number of Catalytically Active Sites for Each Catalyst. *ACS Catal.* **2012**, *2* (9), 1967–1975. https://doi.org/10.1021/cs300330c.
(49) Bayram, E.; Linehan, J. C.; Fulton, J. L.; Roberts, J. A. S.; Szymczak, N. K.; Smurthwaite, T. D.; Özkar, S.; Balasubramanian, M.; Finke, R. G. Is It Homogeneous or Heterogeneous Catalysis Derived from $[RhCp^*Cl_2]_2$? *In Operando* XAFS, Kinetic, and Crucial Kinetic Poisoning Evidence for Subnanometer Rh_4 Cluster-Based Benzene Hydrogenation Catalysis. *J. Am. Chem. Soc.* **2011**, *133* (46), 18889–18902. https://doi.org/10.1021/ja2073438.

Acknowledgements

We would like to acknowledge all members of the Surendranath lab for valuable discussions. We would also like to thank Prof. Richard Finke, Prof. Shannon Stahl, and Prof. Prashant Deshlahra, for valuable discussions.

Funding

Support for liquid phase studies in this work was provided by the National Science Foundation through a CCI Phase I grant for the Center for Interfacial Ionics, under award no. 2221599. Support for gas phase studies in this work was provided by the Gordon and Betty Moore Foundation, under grant ID: GBMF11510. D.M.H. and K.L. acknowledge support from the National Science Foundation Graduate Research Fellowship under grant no. 1745302

Author contributions

D.M.H. and K.L. contributed to project conceptualization, experimental methodology, data collection and analysis, and manuscript preparation. B.Y.T. contributed to project conceptualization, experimental methodology and manuscript review. Y.S. contributed to project conceptualization, experimental methodology and manuscript preparation.

Competing interests

The authors report no competing interests

Data and materials availability

All data are available in the main text or the supplementary materials.